Magnetic Resonance in Medicine 42:425–429 (1999)

Pseudo-Continuous Arterial Spin Labeling Technique for Measuring CBF Dynamics With High Temporal Resolution

Afonso C. Silva* and Seong-Gi Kim

Cerebral blood flow (CBF) can be measured noninvasively with nuclear magnetic resonance (NMR) by using arterial water as an endogenous perfusion tracer. However, the arterial spin labeling (ASL) techniques suffer from poor temporal resolution due to the need to wait for the exchange of labeled arterial spins with tissue spins to produce contrast. In this work, a new ASL technique is introduced, which allows the measurement of CBF dynamics with high temporal and spatial resolution. This novel method was used in rats to determine the dynamics of CBF changes elicited by somatosensory stimulation with a temporal resolution of 108 ms. The onset time of the CBF response was 0.6 ± 0.4 sec (mean ± SD) after onset of stimulation ($n = 10$). The peak response was observed 4.4 ± 3.7 sec (mean ± SD) after stimulation began. These results are in excellent agreement with previous data obtained with invasive techniques, such as laser-Doppler flowmetry and hydrogen clearance, and suggest the appropriateness of this novel technique to probe CBF dynamics in functional and pathological studies with high temporal and spatial resolution. Magn Reson Med 42:425–429, 1999.

Key words: cerebral blood flow; arterial spin labeling; echo-planar imaging; functional brain mapping

The measurement of cerebral blood flow (CBF) is a very important way of assessing tissue viability, metabolism, and function. Furthermore, dynamic measurements of CBF can elucidate the mechanisms of CBF regulation and determine the dynamic behavior of the neuronal responses induced by functional stimulation, drugs, or treatments. Dynamic CBF responses have been mainly studied by laser-Doppler flowmetry (LDF) techniques (1–6). However, this technique is invasive, is not quantitative and has poor spatial resolution.

CBF can be measured noninvasively with NMR by using arterial water as a perfusion tracer (7–13). The arterial spin labeling (ASL) techniques can be implemented with either pulsed labeling (8,10,12), or continuous labeling (7,11,13). The pulsed labeling methods use single or multiple RF pulse(s) to label arterial blood water spins. The continuous ASL technique uses a long radio frequency (RF) pulse in the presence of a longitudinal field gradient to label the arterial spins according to the principles of adiabatic fast passage (14). Proper perfusion contrast is achieved when enough time is allowed for the labeled spins to travel into the region of interest and exchange with tissue spins. This exchange causes a net change in tissue magnetization that is proportional to CBF. In addition, it is necessary to acquire two images, usually in an interleaved manner, to determine CBF: one with spin labeling and another as a control. Thus, the ASL methods suffer from poor temporal resolution, which is typically on the order of a few seconds (8,10,13).

In order to obtain dynamic CBF changes with high temporal and spatial resolution, we devised a novel NMR method, which uses a pseudo-continuous version of the ASL technique. In this new approach, two separate experiments are performed: one with spin labeling and the other as a control. The temporal resolution of the CBF measurements is enhanced by using a short ASL RF pulse in conjunction with an ultra-fast imaging sequence. In the present study, we describe the principles and the details of implementation of the pseudo-continuous ASL technique. This technique was used to investigate the temporal behavior of CBF changes, with a temporal resolution of about 100 msec, during somatosensory stimulation (15) in rat.

THEORY

To increase the temporal resolution, CBF-weighted images have to be acquired separately, either with or without ASL. Between the acquisition of two consecutive images with a short repetition time (TR), and a small RF flip angle of θ degrees, arterial spin labeling is achieved by a labeling RF pulse of length TL. According to this scheme, labeling of the arterial spins can be done with a duty-cycle $k = TL/TR$. If TL is not too short compared to TR, the duty-cycle k is high enough to preserve the sensitivity of the continuous ASL technique.

Since RF pulses are rapidly repeated to obtain high temporal resolution, the flip angle θ will determine how fast the longitudinal tissue magnetization M_z reaches the steady state condition. Assuming the transverse magnetization is completely spoiled after the end of each image, the longitudinal tissue magnetization (without labeling) after n RF pulses is (16):

$$M_z(n \times TR) = \frac{M_0(1 - e^{-TR/T_{1app}})}{1 - \cos\theta \cdot e^{-TR/T_{1app}}} + \frac{M_0(1 - \cos\theta)\, e^{-TR/T_{1app}}}{1 - \cos\theta \cdot e^{-TR/T_{1app}}} \cdot \cos^n\theta \cdot e^{-nTR/T_{1app}} \quad [1]$$

where M_0 is the longitudinal magnetization at the fully relaxed state, and T_{1app} is the longitudinal relaxation time, including the effects of CBF (7,17). The first term in Eq. [1] represents the longitudinal magnetization at the steady state condition, and the second term represents the dy-

Center for Magnetic Resonance Research, Department of Radiology, University of Minnesota Medical School, Minneapolis, Minnesota.

Grant sponsor: National Institutes of Health; Grant numbers: RR08079; N538295; Grant sponsor: Whitaker Foundation.

*Correspondence to: Afonso C. Silva, Ph.D., Center for Magnetic Resonance Research, University of Minnesota Medical School, 2021 6th Street SE, Minneapolis, MN 55455. E-mail: afonso@cmrr.umn.edu

Received 18 February 1999; revised 20 May 1999; accepted 3 June 1999.

namic evolution of M_z from the fully relaxed condition to the steady state condition.

The behavior of the tissue magnetization under the above-described experimental conditions can be simulated by numerical solution of the Bloch equations, modified to include the effects of perfusion (17–19). Figure 1a shows the results of such simulation, using TR = 108 msec, T_1 = 1.9 sec, CBF =1.0 ml g^{-1} min^{-1}, and two values for the flip angle θ, 11.25° and 22.5°. Due to rapid RF pulsing, the tissue magnetization evolves to a steady-state value—related to the local CBF, and to TR and θ as shown in Eq. [1]—only after a sufficient number of images has been acquired. The evolution under θ = 22.5° occurs faster than using θ = 11.25°, as predicted by the second term in Eq. [1]. However, this faster equilibration of the longitudinal magnetization occurs at the expense of signal-to-noise. A 16-sec perturbation of CBF is initiated at time t = 27 sec, when CBF is doubled almost instantaneously. Similar to the initial part of the magnetization time-course, the longitudinal magnetization cannot accommodate this step change in CBF instantaneously. The longitudinal magnetization only reaches the new steady state value after a few seconds. This change in the magnetization due to the change in CBF also occurs faster at larger flip angles.

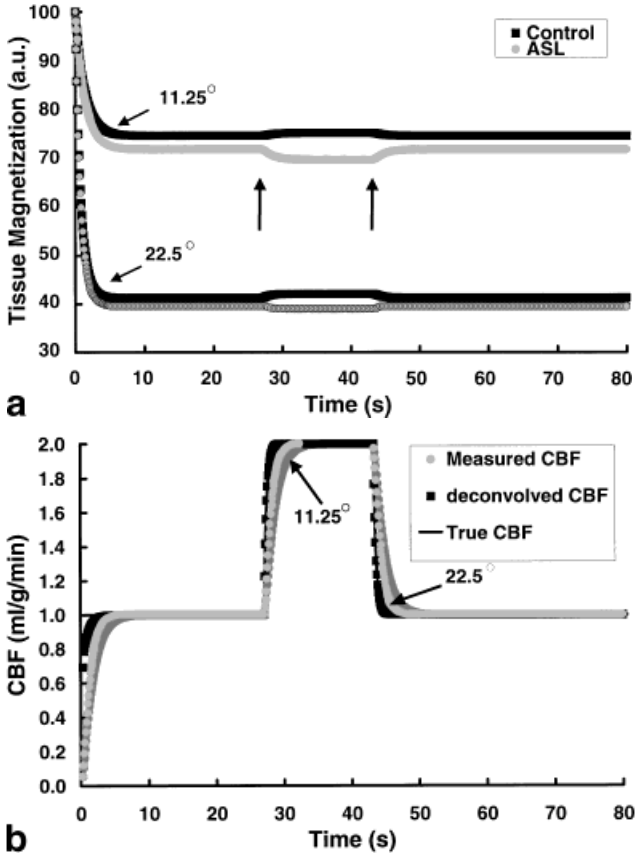

FIG. 1. **a:** Simulation of the behavior of the tissue magnetization in the pseudo-continuous arterial spin labeling method (see Theory). Once the experiment starts, the tissue magnetization evolves to a steady-state value according to Eq. [1]. The rate of evolution of the longitudinal magnetization depends on the repetition time (TR), and on the RF flip angle used to acquire the data. Larger flip angles cause faster evolution of the magnetization. Sudden changes in CBF (vertical arrows) causes a slow evolution of the magnetization to a new steady state value. Changes in T_{1app} due to changes in CBF can also be detected in the control images (inflow effects), but this effect is very small for the parameters used in this work. **b:** Due to the slow changes in tissue magnetization, sudden CBF changes (black line) are convolved with a function which depends on the RF flip angle and on the T_{1app} decay, producing the measured CBF curve (gray circles). A deconvolution process of the measured CBF changes with the magnetization decay curve is necessary to accurately recover the time-course of the intrinsic CBF changes (black squares).

Static CBF Calculation During the Steady State Condition

If changes in CBF occur slowly compared to T_{1app}, CBF images can be formed with a nominal temporal resolution of TR (in this work 108 msec), by pairwise subtraction of the labeled and control images on a pixel-by-pixel basis, according to (17,19):

$$CBF = \frac{\lambda}{T_1} \frac{S_C - S_L}{S_L + (2\alpha - 1)S_C}, \quad [2]$$

where λ is the blood-brain partition coefficient for water, T_1 is the brain tissue longitudinal relation time, S_C is the control image signal intensity, S_L is the labeled image signal intensity, and α is a measure of the efficiency of arterial spin labeling (11,20). Equation [2] neglects the effects of cross-relaxation between brain water and macromolecules. However, it has been shown that this is a small effect (18,19).

The proper determination of quantitative CBF maps requires a correct measure of the degree of arterial spin labeling, α. The definition of α is given by:

$$\alpha = k \cdot \alpha_0 \cdot \exp(\tau / T_{1b}) \quad [3]$$

where α_0 is a measure of the efficiency of arterial spin inversion *at the labeling plane*, τ is the transit time from the labeling plane to the imaging plane, and T_{1b} is the longitudinal relaxation time of arterial blood water. Equation [3] shows that the effect of using the pseudo-continuous arterial spin labeling scheme as described above is to decrease the efficiency of labeling by the duty-cycle factor k.

Dynamic CBF Changes

Once the CBF images are formed according to Eq. [2], an analysis of the temporal characteristics of the CBF time course is desired. For this, a temporal deconvolution of the CBF time-course becomes necessary. This is because instantaneous changes in CBF cause slow variations in the MRI signal. The basic principle of the ASL technique is the transfer of the longitudinal magnetization state of the arterial water spins to the tissue spins (7). This transfer is limited by T_{1app}, by TR, and by the RF flip angle θ, and cannot occur instantly. Therefore, step changes in perfusion (and, consequently, in T_{1app}) are only reflected a few seconds later in the tissue magnetization. This effect is shown in Fig 1b. A simulated step change in perfusion (black line) is only reflected accurately a few seconds later by the MRI measured CBF (gray circles). Notice that the CBF dynamics measured with an RF flip angle θ > 22.5° is closer to the true CBF curve than the one measured using

$\theta = 11.25°$. By performing a deconvolution of the MRI measured CBF signal with the initial magnetization decay curve, as shown in Fig. 1a, this latency in the MRI measured CBF response can be removed. After the deconvolution, the deconvolved CBF time-course (black squares in Fig. 1b) reflects accurately the dynamics of the simulated CBF changes.

MATERIALS AND METHODS

MRI Methods

All images were acquired using a 9.4T/31 cm horizontal magnet (Magnex, UK), interfaced to a Unity INOVA console (Varian, CA). Single-average, single-shot gradient-echo EPI images were obtained using an inplane resolution of 470 × 470 μm^2, slice-thickness = 2 mm, and $TE = 10$ msec, for a total imaging time of 30 msec. Spoiler gradients were applied at the end of the EPI sequence in all three directions to destroy any residual transverse magnetization. The TR time was 108 msec. Inflow effects on the control images (21,22) were reduced by using a tip angle of 11°, smaller than the Ernst angle of 19° calculated using $TR = 108$ msec and $T_1 = 1.9$ sec (23). Single-slice coronal images were obtained covering the somatosensory cortex, about 0–1 mm rostral to bregma.

For continuous ASL, the two coils were arranged such that the RF field of the imaging coil was orthogonal to the RF field of the labeling coil, avoiding interaction (i.e., coupling) between the two coils. The electrical isolation between the two coils when an animal was inside the magnet was greater than 20 dB. Therefore, there was no need for active decoupling schemes (11) between the two coils. The labeling RF pulse was applied to the labeling coil under the presence of a 10 mT/m longitudinal gradient, during $TL = 78$ msec. For the control images the sign of the offset-frequency used for labeling was switched (11).

Animal Preparation

Methods for surgical preparation of the rats have been described in detail previously (11,19) and are summarized below. The MRI studies were conducted in 10 male Sprague-Dawley rats weighing 253 ± 30 g. Surgical procedures were performed under halothane anesthesia (5% induction, 1.5% maintenance). The rats were orally intubated, and catheters were inserted in the left femoral artery and vein. After surgery, the rats were placed in a home-made head holder, and a 1.6-cm diameter surface coil was positioned on top of the head over bregma and secured to the head holder. The animals were then placed in a semi-cylindrical cradle, which contained a small 0.5-cm diameter butterfly labeling coil (11) used for the continuous arterial spin labeling experiments. Care was taken to position the neck of the animal over the labeling coil. The typical separation between the center of the two coils was 2 cm. Rectal temperature was maintained close to 37°C by means of a heated water blanket. Halothane was discontinued, and anesthesia was switched to α-chloralose (80 mg/kg initially, followed by 40 mg/kg every 90 min). Arterial blood pressure was recorded throughout the experiments. Blood gases were adjusted and monitored throughout the experiments. Arterial blood pH was 7.34 ± 0.08, $PaCO_2$ was 37.0 ± 3.9 mm Hg, and PaO_2 was 170 ± 53 mm Hg.

For forepaw stimulation, two needle electrodes were inserted under the skin of either the right or the left forepaw (in the space between digits 2 and 3 and between digits 4 and 5). Stimulation parameters were: current intensity 1.5 mA, frequency 3 Hz, and pulse duration 0.3 msec. These parameters were chosen to produce the greatest CBF changes without inducing arterial blood pressure changes (24). Stimulations were time-gated to the image acquisition. First, 250 baseline images (27 sec) were acquired in the resting state. Then, 200 images (21.6 sec) were acquired during forepaw stimulation. Finally, 450 images (48.6 s) were acquired without stimulation. Consecutive stimulation epochs were separated by a resting period of at least 5 min.

Data Analysis

CBF images were formed with a nominal temporal resolution of 108 msec by pairwise subtraction of the labeled and control images on a pixel-by-pixel basis, according to Eq. [2]. In this work, we used $\lambda = 0.9$ (25) and $T_1 = 1.9$ sec (23). The degree of labeling efficiency as defined by Eq. [3] can be measured by either one of two ways: (i) estimating α_0, τ, and T_{1b}, and calculate α according to Eq. [3] or (ii) measuring the degree of spin inversion α_1 [$= \alpha_0 \exp(-\tau/T_{1b})$] *at the imaging plane*, and then calculate $\alpha = k\alpha_1$ from Eq. [3]. We took the latter approach. Following the same procedures described in (11), we measured $\alpha_1 = 0.81 \pm 0.03$ SD ($n = 7$). This value is in excellent agreement with the value of 0.82 reported in (11). Therefore, the effective degree of spin labeling α was estimated to be $\alpha = 0.59$.

CBF images were processed using a boxcar cross-correlation method (26). Activation maps were generated by thresholding to a minimum cross-correlation coefficient of 0.3 (26). The minimum cluster size for an active region was four pixels (27) ($P > 1.5 \times 10^{-7}$).

The temporal characteristics of CBF changes during forepaw stimulation were determined from region of interest (ROI) analysis. Typically, 9 pixels in the contralateral somatosensory area were chosen, based on the activation maps. Once the CBF time-courses were obtained from a 9-pixel ROI, an analysis of the temporal characteristics was performed. The temporal deconvolution of the CBF time-course was performed using dedicated software written in MATLAB (The Math Works, Inc.). Deconvolved CBF time-courses were analyzed using a polynomial fit. The time origin was set to the onset of stimulation. The fit was constrained from 1 sec before to 20 sec after the onset of stimulation. CBF time-courses were individually fitted and response times were recorded. The onset of response was defined as the latency from the stimulus onset to the first data point above one standard deviation of the baseline value. We also recorded the time-to-peak. All numbers are given as mean ± SD.

RESULTS

Figure 2a shows a typical CBF activation map (cross-correlation coefficient ≥ 0.3) resulting from stimulation of the left forepaw, overlaid onto the EPI anatomical image. The coronal image is viewed in radiological coordinates (right hemisphere is displayed on the left-hand side of the

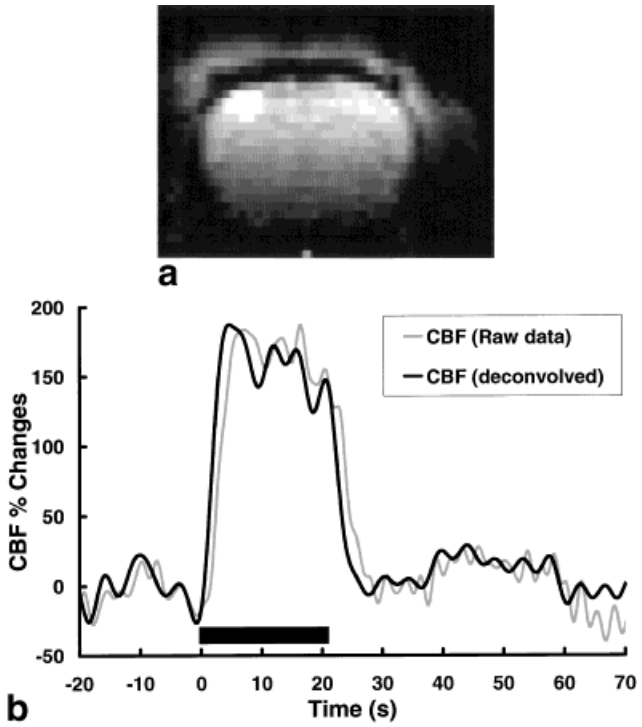

FIG. 2. **a:** Anatomical coronal image of the rat brain. The CBF activation map resulting from a boxcar cross-correlation with the time-course of the stimulation is overlaid onto the anatomical image. **b:** Time-course of a 9-pixel ROI placed on the center of the active areas of the CBF map shown in **a**. The MRI-measured CBF curve (gray) was deconvolved to produce the true CBF curve (black).

image). Activation is confined to a well-defined region of the contralateral somatosensory cortex.

Figure 2b shows the CBF time-course of a 9-pixel ROI placed on the center of the active area in the CBF map shown in Fig. 2a. The curves plotted in Fig. 2b represent the MRI-estimated CBF time-course (gray), and the deconvolved CBF time-course (black). The stimulation period is indicated by the horizontal bar. The origin of the time axis was set to the onset of stimulation. The MRI-estimated CBF curve was deconvolved with the initial 10 sec of the control magnetization decay, generating the deconvolved CBF signal. It can be clearly seen how the CBF response measured with MRI is delayed with respect to the deconvolved curve. It can be noticed from Fig. 2b that the deconvolution adds oscillatory noise to the resulting curve. However, the CBF changes elicited by this model of activation are very robust, to the point that the results presented here are not compromised by the additional noise introduced by the deconvolution process. Therefore, we herein refer to the deconvolved CBF time-course simply as the CBF response; all subsequent temporal analysis and results presented in this work pertain to this deconvolved signal. For this particular rat, the onset of the CBF response started 0.5 sec after stimulation begun, and reached its maximum response of 180% at 3.5 sec. Shortly after the end of stimulation, CBF returned to baseline.

The calculated CBF baseline value obtained from all animals during the prestimulation resting period, according to Eq. [2], was 1.18 ± 0.44 ml g^{-1} min^{-1}. The averaged CBF increase obtained from all animals was $87 \pm 63\%$. This data is in good agreement with our previous report (24). The average onset time of the CBF response was 0.6 ± 0.4 sec following onset of stimulation. The averaged time-to-peak was 4.4 ± 3.7 sec.

DISCUSSION

We have developed a high temporal resolution MRI technique for determining the dynamics of CBF changes with high spatial resolution. Currently, laser-Doppler flowmetry is used for dynamic studies of CBF. However, this technique has higher sensitivity to the surface of the cortex and does not provide quantitative CBF values. Our MRI technique is noninvasive, quantitative, and provides high spatial and temporal resolution. The temporal resolution achieved in this work was 108 msec, and even higher temporal resolution could be achieved at the expense of signal-to-noise (due to the short repetition time and small flip-angle), and labeling efficiency (k factor in Eq. [3]). In fact, the degree of labeling α as expressed by Eq. [3] contains the three major parameters that could limit the usefulness of our technique: They are the transit time τ, the T_1 of blood (T_{1b}), and the labeling duty-cycle factor, k. In this work, we benefited from the short transit-time of rats [$\approx$200 msec (20)], and from the long T_{1b} at 9.4T [$T_{1b} = 2.3$ sec (23)]. Longer transit-times (such as the ones found in larger animals and humans), or shorter T_{1b} if the experiments are performed at lower magnetic field strengths would reduce further the degree of labeling α, and decrease the sensitivity of our technique. The technique can easily be adapted to multi-slice schemes. However, this would happen at the expense of labeling duty-cycle. Another potential limitation with this technique is the deconvolution of the MRI signals to obtain the true dynamics of CBF changes. The deconvolution function must be obtained from the dynamic evolution of the longitudinal magnetization from equilibrium to steady state, prior to inducing any CBF changes, to account both for the T_{1app} decay as well as for the effect of the RF flip angle θ.

One drawback of this technique is the necessity to acquire two sets of images separately. This procedure raises concern over whether the two different stimulation epochs elicit the same hemodynamic response. We tried to minimize this concern by careful control of the experimental conditions: arterial blood pressure and blood gases were monitored and maintained at normal values; the stimulation parameters were chosen to produce robust CBF increases in the contralateral somatosensory cortex, without eliciting arterial blood pressure changes or activation of the ipsilateral cortex (24); and last, but not least, enough time was allowed between the two experiments to avoid interference of one stimulation epoch over the next one (24).

Our data shows that the observed signal changes induced by forepaw stimulation were well above the pixel noise level, and therefore, easy to detect without any signal averaging. Our data shows CBF starts to increase 0.6 ± 0.4 sec after the onset of stimulation, and peaks at 4.4 ± 3.7 sec. Dynamic CBF changes during somatosensory stimulation in rats have been performed by other groups. Using the hydrogen clearance method, Moskalenko et al. observed CBF changes in a whisker barrel stimulation model to

initiate in less than 1 sec (28). Also using a whisker barrel stimulation model, Lindauer et al. showed CBF reached peak values 2–3 sec after onset of stimulation (29). In a recent work, Detre et al. used LDF to look at the dynamics of CBF changes during forepaw stimulation in rat (6). Their results show that the onset of response to a 16 sec, 1 mA, 5 Hz stimulation period is 1.47 ± 0.21 sec, while the time-to-peak is 4.34 ± 0.21 sec. Although their observed time-to-peak is similar to our findings, their data suggest a much later CBF response than the one reported here. This could be due, in part, to the fact that LDF is more sensitive to superficial variations in CBF, which could be dynamically different from the CBF response shown here from deep layers of the cortex. Furthermore, the stimulation parameters were different, and likely to elicit a different dynamic response as the one reported in this work.

In summary, we devised a technique that allows the measurement of CBF relative changes to a brain functional paradigm with high temporal resolution. We used this technique to characterize the temporal response of CBF to somatosensory stimulation in rat. When used with T_2^* sensitive techniques, such as EPI, the technique has the potential to detect simultaneous BOLD and CBF changes elicited by neuronal activation. This is the subject of our forthcoming companion article (30).

ACKNOWLEDGMENTS

The authors thank Dr. Emmanuel L. Barbier and Dr. Alan P. Koretsky for stimulating discussions. The 9.4 T facility was funded in part by the Keck Foundation.

REFERENCES

1. Haberl RL, Heizer ML, Marmarou A, Ellis EF. Laser-Doppler assessment of brain microcirculation: effect of systemic alterations. Am J Physiol 1989;256:H1247–H1254.
2. Dirnagl U, Kaplan B, Jacewicz M, Pulsinelli W. Continuous measurement of cerebral cortical blood flow by laser-Doppler flowmetry in a rat stroke model. J Cereb Blood Flow Metab 1989;9:589–596.
3. Iadecola C, Reis DJ. Continuous monitoring of cerebrocortical blood flow during stimulation of the cerebellar fastigial nucleus: a study by laser-Doppler flowmetry. J Cereb Blood Flow Metab 1990;10:608–617.
4. Ngai AC, Meno JR, Winn HR. Simultaneous measurements of pial arteriolar diameter and laser-Doppler flow during somatosensory stimulation. J Cereb Blood Flow Metab 1995:15:124–127.
5. Malonek D, Dirnagl U, Lindauer U, Yamada K, Kanno I, Grinvald A. Vascular imprints of neuronal activity: relationships between the dynamics of cortical blood flow, oxygenation, and volume changes following sensory stimulation. Proc Natl Acad Sci. (USA) 1997;94: 14826–14831.
6. Detre JA, Ances BM, Takahashi K, Greenberg JH. Signal averaged laser Doppler measurements of activation-flow coupling in the rat forepaw somatosensory cortex. Brain Res 1998;796:91–98.
7. Williams DS, Detre JA, Leigh JS, Koretsky AP. Magnetic resonance imaging of perfusion using spin inversion of arterial water. Proc Natl Acad Sci (USA) 1992;89:212–216.
8. Kwong KK, Belliveau JW, Chesler DA, Goldberg IE, Weisskoff RM, Poncelet BP, Kennedy DN, Hoppel BE, Cohen MS, Turner R. Dynamic magnetic resonance imaging of human brain activity during primary sensory stimulation. Proc Natl Acad Sci (USA) 1992;89:5675–5679.
9. Edelman RR, Siewert B, Darby DG, Thangaraj V, Nobre AC, Mesulam MM, Warach S. Qualitative mapping of cerebral blood flow and functional localization with echo-planar MR imaging and signal targeting with alternating radio frequency. Radiology 1994;192:513–520.
10. Kim SG. Quantification of relative cerebral blood flow change by flow-sensitive alternating inversion recovery (FAIR) technique: application to functional mapping. Magn Reson Med 1995;34:293–301.
11. Silva AC, Zhang W, Williams DS, Koretsky AP. Multi-slice MRI of rat brain perfusion during amphetamine stimulation using arterial spin labeling. Magn Reson Med 1995;33:209–214.
12. Wong EC, Buxton RB, Frank LR. Implementation of quantitative perfusion imaging techniques for functional brain mapping using pulsed arterial spin labeling. NMR Biomed 1997;10:237–249.
13. Alsop DC, Detre JA. Multisection cerebral blood flow MR imaging with continuous arterial spin labeling. Radiology 1998;208:410–416.
14. Dixon WT, Du LN, Faul DD, Gado MH, Rossnick S. Projection angiograms of blood labeled by adiabatic fast passage. Magn Reson Med 1986:3:454–462.
15. Ueki M, Mies G, Hossmann KA. Effect of alpha-chloralose, halothane, pentobarbital and nitrous oxide anesthesia on metabolic coupling in somatosensory cortex of rat. Acta Anaesthesiol Scand 1992;36:318–322.
16. Gao JH, Holland SK, Gore JC. Nuclear magnetic resonance signal from flowing nuclei in rapid imaging using gradient echoes. Med Phys 1988;15:809–814.
17. Zhang W, Williams DS, Detre JA, Koretsky AP. Measurement of brain perfusion by volume-localized and cross-relaxation. Magn Reson Med 1992;25:362–371.
18. Zhang W, Silva AC, Williams DS, Koretsky AP. NMR measurement of perfusion using arterial spin labeling without saturation of macromolecular spins. Magn Reson Med 1995;33:370–376.
19. Silva AC, Zhang W, Williams DS, Koretsky AP. Estimation of water extraction fractions in rat brain using magnetic resonance measurement of perfusion with arterial spin labeling. Magn Reson Med 1997:37:58–68.
20. Zhang W, Williams DS, Koretsky AP. Measurement of rat brain perfusion by NMR using spin labeling of arterial water: in vivo determination of the degree of spin labeling. Magn Reson Med 1993:29:416–421.
21. S. G. Kim, K. Hendrich, Hu X, Merkle H, Ugurbil K. Potential pitfalls of functional MRI using conventional gradient-recalled echo techniques. NMR Biomed 1994;7:69–74.
22. Frahm J, Merboldt KD, Hanicke W, Kleinschmidt A, Boecker Brain or vein — oxygenation or flow? On signal physiology in functional MRI of human brain activation. NMR Biomed 1994;7:45–53.
23. Tsekos NV, Zhang F, Merkle H, Nagayama M, Iadecola C, Kim SG. Quantitative measurements of cerebral blood flow in rats using the FAIR technique: correlation with previous iodoantipyrine autoradiographic studies. Magn Reson Med 1998:39:564–573.
24. Silva AC, Lee S-P, Yang G, Iadecola C, Kim S-G. Simultaneous BOLD and CBF Functional MRI during Forepaw Stimulation in Rat. J Cereb Blood Flow Metab 1999, in press.
25. Herscovitch P, Raichle ME. What is the correct value for the brain-blood partition coefficient for water? J Cereb Blood Flow Metab 1985;5:65–69.
26. Bandettini PA, Jesmanowicz A, Wong EC, Hyde JS. Processing strategies for time-course data sets in functional MRI of the human brain. Magn Reson Med 1993;30:161–173.
27. Forman SD, Cohen JD, Fitzgerald M, Eddy WF, Mintun MA, Noll DC. Improved assessment of significant activation in functional magnetic resonance imaging (fMRI): use of a cluster-size threshold. Magn Reson Med 1995;33:636–647.
28. Moskalenko YE, Dowling JL, Liu D, Rovainen CM, Semernia VN, Woolsey TA. LCBF changes in rat somatosensory cortex during whisker stimulation monitored by dynamic H2 clearance. Int J Psychophysiol 1996;21:45–59.
29. Lindauer U, Villringer A, Dirnagl U. Characterization of CBF response to somatosensory stimulation: model and influence of anesthetics. Am J Physiol 1993;264:H1223–H1228.
30. Silva AC, Lee S-P, Iadecola C, Kim S-G. Early temporal characteristics of CBF and deoxyhemoglobin changes during somatosensory stimulation. J Cereb Blood Flow Metab 1999, in press.